Korean J. Chem. Eng., **24**(5), 847-850 (2007)

SHORT COMMUNICATION

Energetic surface heterogeneity of nanocrystalline TiO_2 films for dye-sensitized solar cells

Jae-Wook Lee, Kyung-Jun Hwang*, Wang-Geun Shim, Kyung-Hee Park***, Hal-Bon Gu*** and Kyu-Hyuk Kwun†**

Department of Chemical and Biochemical Engineering, Chosun University, Gwangju 501-759, Korea
*Department of Environmental and Chemical Engineering, Seonam University, Namwon 590-170, Korea
**Faculty of Applied Chemical Engineering, ***Department of Electric Engineering,
Chonnam National University, Gwangju 500-757, Korea
(*Received 13 November 2006 • accepted 1 February 2007*)

Abstract−Dye sensitized solar cells (DSSCs) have been receiving significant attention because they have many advantages compared to conventional organic solar cells. It has been known that the photovoltaic characteristics of DSSC are highly dependent on the adsorption properties of dyes on TiO_2 films. To analyze the surface heterogeneity of TiO_2 surfaces, single-phase anatase nanocrystallite titanium films were prepared by sol-gel method using the hydrolysis reaction of titanium tetraisopropoxide under acidic condition and characterized by XRD, FE-SEM and BET analysis. The adsorption energy distribution functions were calculated by the generalized nonlinear regularization method. It was found that the shape and the intensity of the adsorption energy distribution curve determined were highly related with the physical properties (i.e., geometrical heterogeneity) and chemical characteristics (i.e., energetic heterogeneity) of nanocrystalline TiO_2 for DSSC.

Key words: Adsorption Energy Distribution Functions, Dye-sensitized Solar Cell, TiO_2 Film

INTRODUCTION

Compared to conventional silicon-type and organic solar cells, dye sensitized solar cells (DSSCs) have been extensively investigated due to their many advantages [1,2]. Among many metal oxides, nanocrystalline titania materials have been extensively studied because of their interesting physical and chemical properties [3]. To achieve high cell performance, a higher surface area and efficient interfacial charge transfer of TiO_2 is required because the solar cell performance includes overall conversion efficiency, fill factor, open-circuit voltage and short-circuit current of the TiO_2/dye sensitized nanocrystalline. TiO_2 solar cell is highly dependent on the adsorption quantity of dye molecules. Recently, it has been pointed out that further work on the design and optimization of nanostructured materials and the analysis of the electron transport dynamics should be conducted to enhance the low energy conversion efficiency of DSSC. Although there have been many studies on the synthesis and characterization of TiO_2 nanocrystallites as well as the development of synthetic dyes, systematic studies on the influence of adsorption states between dye molecules and TiO_2 films on the power conversion efficiency of DSSC are very limited. Prior to the investigation of the influence of Ru(II) dye adsorption properties on the conversion efficiency of DSSC, this work focuses on the evaluation of the adsorption energy distribution functions of TiO_2 using nitrogen isotherm data by a generalized nonlinear regularization method. The adsorption energy distribution functions will offer the fundamental and informative data to fully understand the surface heterogeneity of the nanostructured TiO_2 materials.

EXPERIMENTAL

A colloidal TiO_2 suspension was prepared by the hydrolysis of titanium-tetraisopropoxide (TTIP, Junsei Chemical Co., >98% purity). TTIP was used as the main starting material without further purification. Then, the TTIP was slowly dropped in ethanol at room temperature for 5 min. Drop-wise addition of hydrochloric acid solution into the TTIP solution was conducted for 24 h under vigorous stirring condition (>500 rpm). The suspension was then ultrasonicated at room temperature for 1 h and centrifuged at 4 °C and 8,000 rpm for 20 min. The white precipitate formed was filtered and dried at room temperature for 1 h. The dried TiO_2 particles were calcined at 450 °C for 30 min in air gas flow. For the preparation of TiO_2 thin-film, TiO_2 slurry was prepared by the addition of TiO_2 particles for 3 h at 300 rpm by using a Zr ball mill (Planetary Mono Mill, FRITSCH) with adding of acetyl acetone, poly(ethylene glycol) (MW 400), and Triton X-100, and water. Acetic acid solutions were dropped in the prepared paste solution and stirred for 3 h. Finally, a TiO_2 film was fabricated by coating a precursor paste onto the fluorine-doped SnO_2 conducting glass plates (FTO, 10 Ωcm^{-2}, Asahi glass Co., Japan) by using a squeeze printing technique (adhesive tape was used as spacer of ca. 43 μm thickness) and followed by heating it at 450 °C for 30 min. The crystallinity of synthesized TiO_2 particles was characterized with an X-ray diffractometer (Rigaku, D/MAX-1200) by using a Cu$K\alpha$ X-ray and Ni filter at 35 kV and 15 mA. The film thickness and surface morphology were measured by field-emission scanning electron microscopy (FE-SEM, S-4700, Hitachi). Nitrogen adsorption and desorption isotherms were measured at 77 K with a Micromeritics ASAP 2010 automatic analyzer. Before the measurements, the samples were outgassed for 2 h in the degas port of the adsorption apparatus. The BET surface areas were determined from the adsorption isotherms of nitrogen. In addition, the pore size distributions were also calculated from the adsorption branches of the isotherms by using the Barrett, Joyner, and Halenda (BJH) method.

†To whom correspondence should be addressed.
E-mail: khkwun@chosun.ac.kr

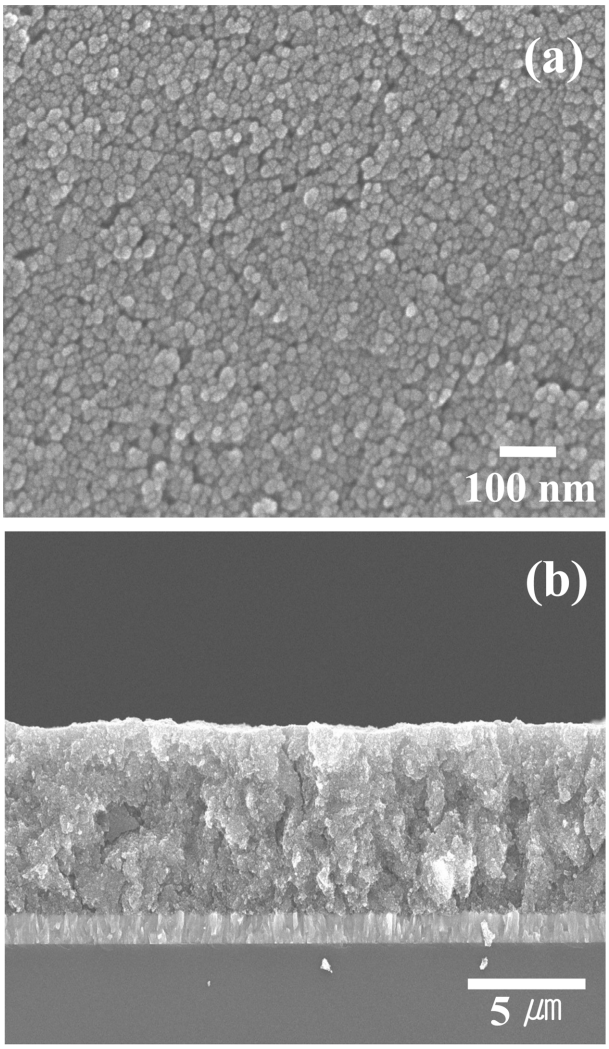

Fig. 1. FE-SEM images of (a) surface and (b) cross-sectional of TiO_2 films.

RESULTS AND DISCUSSION

To date, P-25 (Degussa) with a mixture of anatase and rutile phases (8 : 2) has been extensively used in DSSC study. In addition, many researchers have addressed that anatase TiO_2-based solar cells exhibit higher photovoltaic characteristics compared to rutile TiO_2-based solar cells because of higher surface area (i.e., higher amount of dye adsorbed) [4]. It was found from XRD patterns that titania particles fabricated in this work are only single-phase anatase nanocrystallites without rutile (not shown here). Fig. 1 exhibits the FE-SEM images of surface morphology and the cross-section of TiO_2 thin films coated on FTO glass. The TiO_2 spherical nanoparticles (ca. 10-20 nm) are well distributed and the film thickness was approximately 10 μm. For comparison purpose, the physico-chemical properties of commercialized P-25 and synthesized TiO_2 are listed in Table 1. The surface area determined nitrogen isotherm data was found to be in the range of 52-70 m^2 g^{-1} (Fig. 2a) and the average pore size calculated by BJH method was in the range of 8.3-9.9 nm (Fig. 2b). A slight increase of surface area of TiO_2 synthesized in this work compared to P-25 is attributed to the development of mesopores by acetic acid treatments.

Table 1. Physical properties of TiO_2

Samples	BET surface area [m^2/g]	Pore volume [cm^3/g]	Average pore size [nm]
A (Degussa)[a]	40	0.29	31.2
B (this work)[b]	52	0.14	8.3
C (this work)[c]	63	0.16	9.4
D (this work)[d]	70	0. 20	9.8

[a]P-25 TiO_2 film (Degussa) with no acid treatment.
[b]TiO_2 film with no acid treatment.
[c]TiO_2 film with acetic acid treatment (0.5 M).
[d]TiO_2 film with acetic acid treatment (1.0 M).

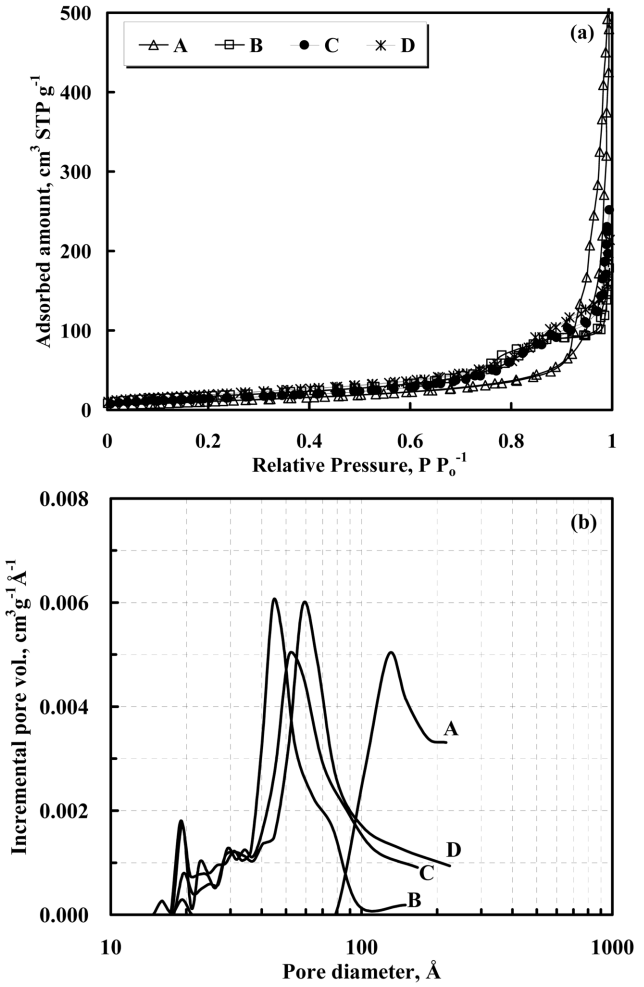

Fig. 2. Nitrogen adsorption and desorption isotherms (a) and pore size distribution functions (b) of P-25 film and synthesized TiO_2 film.

The fill factor (FF) and overall energy efficiency (η) for nanocrystalline DSSC are determined by photocurrent-voltage (I-V) [1]:

$$\eta(\%) = \frac{P_{out}}{P_{in}} \times 100 = \frac{I_{max} \times V_{max}}{P_{in}} \times 100 = \frac{I_{SC} \times V_{OC} \times FF}{P_{in}} \times 100 \quad (1)$$

where I_{SC} is the short-circuit current density ($mAcm^{-2}$), V_{OC} is the open-circuit voltage (V), P_{in} is the incident light power, and I_{max} (mA

cm^{-2}) and V_{max} (V) are the current density and voltage in the I-V curve at the point of maximum power output. The order of the photocurrent densities increased with the adsorption amount of dye molecules (i.e., N3, N719 and black dyes). From our previous work [5], we found that high adsorption capacity of TiO_2 with low charge transfer resistance yields a superior I_{SC} of DSSC. As a continuous work, therefore, it is essential to understand the energetic and structural heterogeneity of TiO_2 surfaces by using nitrogen adsorption data for the systematic analysis of the adsorption properties between dye molecule and TiO_2 surfaces.

It has been known that chemical and geometrical heterogeneities show the unique sorption properties of porous materials. Geometrical heterogeneity comes from the differences in size and shape of pores, while chemical heterogeneity is associated with different functional groups and various surface defects on a surface. The heterogeneity properties of solid adsorbents can be described by their so-called adsorption energy distribution functions [6]. Adsorption energy distributions have been extensively applied for characterizing the numerous adsorption systems and understanding the surface energy heterogeneities. The fundamental adsorption integral equation for energetically heterogeneous solid surfaces is given as follows [7-9]:

$$\theta(p) = \int_{E_{min}}^{E_{max}} \theta(p,E) \cdot F(E) \cdot dE \quad (2)$$

where p is the equilibrium pressure, E is the adsorption energy, F(E) is the adsorption energy distribution function, θ(p, E) is a local adsorption isotherm with an adsorption energy, θ(p) is the experimental adsorption isotherm data. The adsorption integral equation is the well-known linear Fredholm integral equation of the first kind, and the calculation of adsorption energy distribution is an ill-posed problem [10]. For the current work, we applied the generalized nonlinear regularization method based on smoothness constraint (i.e., Tikhonov regularization) and edge preserving regularization methods. The generalized nonlinear regularization method can avoid the difficulties resulting from the ill-posed nature of an adsorption integral equation [11]. Fig. 3 shows the flow chart for the general calculation of adsorption energy distribution [12,13]. Here, proper selection of the local adsorption isotherm equation for the calculation of energy distribution is very important in analyzing the heterogeneous adsorption systems. In this work, the Fowler and Guggenheim equation is used:

$$\theta(p,E) = \frac{K \cdot p \cdot \exp\left(\frac{zw\theta}{k_B T}\right)}{1 + p \cdot \exp\left(\frac{zw\theta}{k_B T}\right)} \quad (3)$$

where T is the absolute temperature, p is the equilibrium pressure, z is the number of closest adjacent molecules in the monolayer, w is the interaction energy between the two nearest neighboring molecules, k_B is the Boltzmann constant, $K=K_0(T)\cdot\exp(E/k_BT)$ is the Langmuir constant, $K_0(T)$ is the pre-exponential factor expressing the partition functions for an isolated molecule [7]. Fig. 4 shows the adsorption energy distribution functions of TiO_2 films formed on the FTO glass. The adsorption energy distribution curves of TiO_2 for samples B-D (Table 2) synthesized in this work exhibited two peaks indicating the existence of energetically two different adsorp-

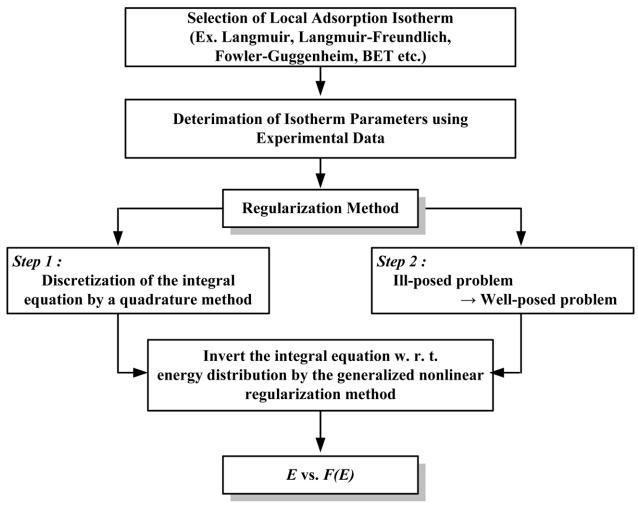

Fig. 3. Flow chart for the general calculation of adsorption energy distribution functions.

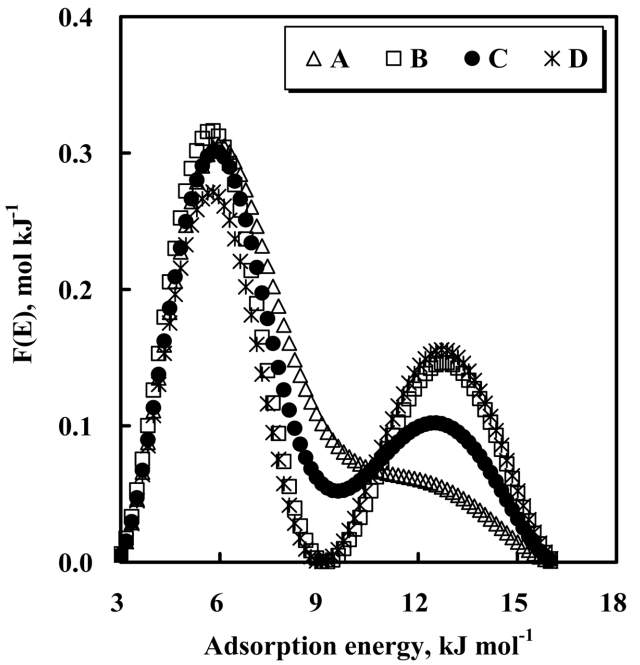

Fig. 4. Adsorption energy distributions of P-25 film and synthesized TiO_2 film.

Table 2. Adsorption energy distribution functions

Samples	1st Peak		2nd Peak	
	Adsorption energy [kJ mol^{-1}]	F(E) [mol kJ^{-1}]	Adsorption energy [kJ mol^{-1}]	F(E) [mol kJ^{-1}]
A	5.80	0.30	-	-
B	5.80	0.32	12.87	0.15
C	5.81	0.31	12.54	0.10
D	5.80	0.27	12.71	0.16

tion sites. The first and second adsorption energy curves were distributed mainly in the range of 3-9 and 9-16 kJ mol^{-1}, respectively. The energy intensity of the first peak is about two times higher than that of the second one. However, the second peak of P-25 was not evident compared to the synthesized TiO_2 samples. The energy distribution peaks proceeded to higher energy with a slight increase of surface area, depending on the acetic acid treatments (0.5 and 1.0 M) because of the micro and mesopore developments on TiO_2 surfaces as well as TiO_2 intraparticles (Table 1). The increase of surface area (i.e., increase in adsorption capacity of dye molecules) will serve for the enhanced energy conversion efficiency of DSSC. It was also found that the shape and the intensity of the adsorption energy distribution curve were highly related with the physical properties (i.e., geometrical heterogeneity) and chemical characteristics (i.e., energetic heterogeneity) of nanocrystalline TiO_2 for DSSC. The results can be successfully applied for the design, synthesis and optimization of nanocrystalline TiO_2 for DSSC because the adsorption energy distribution functions obtained in this work will offer the fundamental and informative data to fully understand the surface heterogeneity of the nanostuctured TiO_2 materials.

CONCLUSION

Nanocrystalline TiO_2 film was formed on the FTO glass for working electrode of DSSC and characterized by XRD, SEM and BET analysis. Compared to the commercialized P-25 (Deggusa), the synthesized TiO_2 shows only single-phase anatase nanocrystallites without rutile. It was also found that TiO_2 films synthesized in this work have highly energetic surface heterogeneities based on the results of the shape and intensity of adsorption energy distribution functions calculated by the generalized nonlinear regularization method. We expect that the results obtained in this work can be widely used in the design and synthesis of nanocrystalline TiO_2 for DSSC.

ACKNOWLEDGEMENT

This work was supported by research funds from Chosun University, 2006.

REFERENCES

1. M. Grätzel, *J. Photochem. Photobiol. C*, **4**, 145 (2003).
2. Md. K. Nazeeruddin, R. Jumphry-Baker, P. Liska and M. Grätzel, *J. Phys. Chem. B*, **107**, 8981 (2003).
3. S. Ngamsinlapasathian, S. Pavasupree, Y. Suzuki and S. Yoshikawa, *Solar Energy Materials & Solar Cells*, **90**, 3187 (2006).
4. N. G. Park, J. V. D. Lagemaat and A. J. Frank, *J. Phys. Chem. B*, **104**, 8989 (2000).
5. J. W. Lee, H. C. Kwang, W. G. Shim, C. Kim, K. S. Yang and H. Moon, *J. Nanoscience and Nanotechnology*, **6**, 3577 (2006).
6. W. Rudzinski and D. H. Everett, *Adsorption of gases on heterogeneous surfaces*, Academic Press, London (1992).
7. M. Jaroniec and R. Madey, *Physical adsorption on heterogeneous solids*, Elsevier, Amsterdam (1988).
8. A. M. Puziy, T. Matynia, B. Gawdzik and O. I. Poddubnaya, *Langmuir*, **15**, 6016 (1999).
9. M. Frere, M. Zinque, K. Berlier and R. Jadot, *Adsorption*, **4**, 239 (1998).
10. M. V. Szombathely, P. Brauer and M. J. Jaroniec, *Comput. Chem.*, **13**, 17 (1992).
11. T. M. Roth, J. Weese and J. Honerkamp, *Comput. Phys. Commun.*, **139**, 279 (2001).
12. J. W. Lee, K. J. Hwang, D. W. Park, K. H. Park, W. G. Shim and S. C. Kim, *J. Nanoscience and Nanotechnology* (in print, 2007).
13. W. G. Shim, H. C. Kang, C. Kim, S. C. Kim, J. W. Lee, C. J. Lee and H. Moon, *J. Nanoscience and Nanotechnology*, **6**, 3583 (2006).